General solutions for quantum dynamical systems driven by time-varying Hamiltonians: applications to NMR

P.-L Giscard, Christian Bonhomme

General solutions for quantum dynamical systems driven by time-varying Hamiltonians: applications to NMR

Pierre-Louis Giscard[a] **and Christian Bonhomme**[b]

[a]Univ. Littoral Côte d'Opale, EA 2597 - LMPA - Laboratoire de Mathématiques Pures et Appliquées Joseph Liouville, F-62228 Calais, France.; [b]Laboratoire de Chimie de la Matière Condensée de Paris, Sorbonne Université, UMR CNRS 7574, 4, place Jussieu, 75252, Paris Cedex 05, France.

This manuscript was compiled on May 9, 2019

Comprehending the dynamical behaviour of quantum systems driven by time-varying Hamiltonians is particularly difficult. Systems with as little as two energy levels are not yet fully understood. Since the inception of Magnus' expansion in 1954, no fundamentally novel mathematical method for solving the quantum equations of motion with a time-varying Hamiltonian has been devised. We report here of an entirely different non-perturbative approach, termed path-sum, which is always guaranteed to converge, yields the exact analytical solution in a finite number of steps for finite systems and is invariant under scale transformations. We solve for the dynamics of all two-level systems as well as of many-body Hamiltonians with a particular emphasis on NMR applications (Bloch-Siegert effect and N-spin systems involving the dipolar Hamiltonian and spin diffusion).

Time-varying Hamiltonian | Path-sum | Analytical and numerical methods | Bloch-Siegert effect | Nuclear Magnetic Resonance | N spins systems and dipolar couplings

Quantum evolution operators: general context and Nuclear Magnetic Resonance background

The unitary evolution operator $\mathsf{U}(t',t)$ describing the time dynamics of quantum systems is defined as the unique solution of Schrödinger's equation with quantum Hamiltonian H, i.e. ($\hbar = 1$)

$$-i\,\mathsf{H}(t')\,\mathsf{U}(t',t) = \frac{d}{dt'}\mathsf{U}(t',t), \qquad [1]$$

and such that $\mathsf{U}(t'=t,\,t) = \mathsf{Id}$ is the identity matrix at all times. Evidently, this operator plays a crucial role at the heart of quantum mechanics, including for spin dynamics in magnetic resonance (Nuclear Magnetic Resonance - NMR, Electronic Paramagnetic Resonance - EPR, Dynamic Nuclear Polarisation - DNP...) (1–3). When the quantum Hamiltonian is time-independent, the evolution operator takes on the mathematically simple and compact form $\mathsf{U}(t',t) = \exp[-i(t'-t)\mathsf{H}]$. In the general case however, and as is typically the case in NMR, the Hamiltonian may be time-dependent and might furthermore not commute with itself at various times, $\mathsf{H}(t)\mathsf{H}(t') - \mathsf{H}(t')\mathsf{H}(t) \neq \mathbf{0}$ for $t' \neq t$. In this situation, the evolution operator no longer has a simple calculable form being rather *formally* given by the action of a time-ordering operator on the exponential of the Hamiltonian, an expression first expounded by Dyson (4) but which is little more than a notation precluding immediate evaluations.

Whereas this problem has been discussed in details in the NMR literature, calculations of the evolution operator remain barely tractable for an in-depth description of spin dynamics. At best, approximate expressions of $\mathsf{U}(t',t)$ are obtained and are only accurate for short times. The same conclusion holds for the so called product representation of the Hamiltonian involving its separation in two parts of equal importance (3). A major breakthrough in the description and understanding of solid state NMR was achieved by the development of Average Hamiltonian Theory (AHT) in the late 1960's by Waugh, Haeberlen and co-workers. AHT relies exclusively on the Magnus expansion (ME) (5) of $\mathsf{U}(t',t)$. Discovered in 1954, this expansion is the last essentially new development in the mathematical theory of time-dependent Hamiltonians. ME was the starting point for a new era in homonuclear decoupling (6, 7) experiments and multiple-quantum spectroscopy (8). The fundamental idea behind the Magnus expansion relies on calculating a matrix whose 'true' exponential gives the evolution operator, a formulation which involves an infinite series of time-dependent nested commutators of the Hamiltonian, mathematically a continuous form of the celebrated Baker-Campbell-Haussdorff formula (9). Nevertheless, higher order terms of the series remain highly cumbersome to write down explicitly so that practically, only low orders of the expansion are useable. Most importantly, ME suffers from severe and incurable problems of convergence as already mentioned by Magnus himself (5) and Maricq in early contributions (10). Quoting Mehring and Weberruss in (3): "*The convergence of this series is of concern and must be considered in special cases*" (!). The specific problem of convergence has been re-investigated in-depth recently (11, 12) and saturated upper bounds for the largest times reachable by ME before divergence have been discovered which severely restrict its use to short times (13). In the more specific case of periodically time-dependent Hamiltonian, such as those encountered in Magic Angle Spinning (MAS) experiments, it is well known that ME suffers from a further two limitations, i.e. the stroboscopic detection of the NMR events, and the impossibility to take into account more than one characteristic period. We mention that in the case of periodic Hamiltonian, Secular Average Theory (SAT) can be applied as well (3)). It implies the separation of constants terms in the Hamiltonian avoiding non-secular contributions in first/higher order terms of the expansion. Using AHT, such terms may lead to erroneous results (14). Ultimately, the SAT approach follows the general

concept developed in ME, with $\mathsf{U}(t',t)$ given by the 'true' exponential of an infinite series of operators.

In the case of periodic Hamiltonian, Floquet theory (FT) holds (15) and implies that the evolution operator takes on the form $\mathsf{U}(t,0) = \mathsf{P}(t)\exp(\mathsf{F}t)$, with $\mathsf{P}(t)$ a periodic time-dependent matrix and F a constant matrix, both of which are determined perturbatively (11). This procedure was first used by Shirley (16), whose fundamental contribution was to apply Floquet theory to the case of linearly polarised excitations in magnetic resonance and to give *low orders* analytical expressions for the Bloch-Siegert effect (17). Shirley's main progress effectively transformed the finite time-dependent Hamiltonian appearing in Schrödinger's equation into an *infinite* but time-independent one via FT. Because the resulting system is infinite, this approach to the evolution operator is inherently perturbative.

In the early 1980's, FT entered the NMR world with innovative applications proposed by Maricq (10) and Vega (18). Most importantly, the severe limitation of stroboscopic observation in AHT is avoided in FT. Nevertheless, a fundamental problem remains in FT, namely the perturbative approach of the Floquet Hamiltonian which is usually performed via van Vleck transformation as an efficient method for block diagonalisation (19).

An effective Floquet operator is consequently obtained for subsequent NMR applications such as design and optimisation of new pulse sequences. Floquet theory is versatile as multiple distinct frequencies can be taken into account simultaneously: multimodal Floquet approaches (20) are now encountered routinely in advanced solid state NMR techniques including RF pulse schemes and macroscopic reorientation of the sample. Among other numerous examples, Floquet theory was successfully applied to recoupling experiments under MAS , hetero- and homonuclear recoupling and decoupling, cross polarisation (based on the heteronuclear dipolar interaction), quadrupolar nuclei ($I > 1/2$) and dynamics under MAS (19). Such experiments correspond to state of the art developments in modern solid state NMR.

Finally, we mention numerical methods: (i) Fer and Magnus-Floquet hybrids proposed recently as potential expansions for the evolution operator (21, 22), (ii) Zassenhaus and Suzuki-Trotter propagator approximations (23–25) The expansions presented above all suffer from various drawbacks including: the divergence of the series at long time; the perturbative nature of the numerical or theoretical approach; the non-avoidable propagation of errors at long time; the failure to find exact solutions even for small, one spin, 2×2 Hamiltonians.

In this contribution, the Path-Sum (PS) (26) method is applied for the very first time to NMR Hamiltonians to determine the corresponding evolution operators $\mathsf{U}(t',t)$. Path-sum is firmly established on three fundamentally novel concepts, insofar never applied within the NMR framework: (i) the representation of $\mathsf{U}(t',t)$ as the inverse of an operator with respect to a newly introduced $*$-product; (ii) a mapping between this inverse, and sums of weighted walks on a graph; and (iii) fundamental results on the algebraic structure of sets of walks which exactly transform any infinite sum of weighted walks on any graph into a single branched continued fraction of finite depth and breadth with finitely many terms. Taken together, these three results imply that, for finite dimensional Hamiltonians, any entry or block of entries of $\mathsf{U}(t',t)$ has a finite, exact, analytical expression in terms of $*$-products and inverses of time-dependent *functions* (rather than matrices). These inverses are themselves determined by unconditionally convergent analytical series or can be found via numerical tools pertaining to linear Volterra integral equations of the second kind with separable kernels. Since every piece of the evolution operator is obtained exactly after a finite number of operations, the method is necessarily convergent. As a corollary, path-sum yields a non-perturbative formulation of $\mathsf{U}(t',t)$, as will be illustrated below with the Bloch-Siegert effect. Further properties of path-sums ensures its scalability to multi-spin systems, for example allowing it to recover the exact dynamics of an entire system from the separate, isolated, evolutions of any chosen collection of its sub-systems.

We may put path-sum in a broader physical context by quoting R. P. Feynman (27): "*With application to quantum mechanics, path integrals suffer most grievously from a serious defect. They do not permit a discussion of spin operators or other such operators in a simple and lucid way*". From our point of view, path-sum precisely achieves what path-integrals could not for spin systems and go further by performing formal resummations on the infinitely many diagrams. Indeed, in the Hamiltonian formalism of spin systems, the quantum state space takes on the form of a discrete graph and its walks, weighted by the energy functional, are the analogs of the Feynman diagrams, all of which are re-summed via a single finite continued fraction over a few *prime* walks. As a corollary, each of the finitely many term of the path-sum continued fraction represents a fundamental physical process from which all possible processes stem via nestings (insertion of a process into another). While these interpretations are correct and appealing, path-sum's validity is independent from quantum theory and physics in general: it is rather a fundamental property of graph walks valid for even the most abstract systems of coupled linear differential equations with non-constant coefficients. Overall, it appears that the present work is the first fundamentally new approach to the problem of simulating quantum dynamics induced by time-varying Hamiltonians since Magnus' 1954 seminal results.

This article is structured as follows. We first give a concise presentation of the rigorous mathematical background of (26) culminating in the path-sum formulation of quantum dynamics. The fundamental scalability property of path-sum is introduced as well. In a second part, we detail four applications in connection with general quantum theory and then more specifically with NMR. The first one provides the general solution of Schrödinger's equation for any 2×2 time-dependent Hamiltonian, a problem of central importance in quantum computing. We demonstrate the use of the solution on a test model, that of a circularly polarised RF excitation in the laboratory frame. Indeed, the exact expression of $\mathsf{U}(t',t)$ is known thanks to a transformation into the rotating frame, yet none of the existing general purpose methods such as Magnus expansion or Floquet theory recovers it exactly. In contrast, we show that path-sum arrives at the analytical solution. Second, we solve the much more complex case of lin-

Author contributions: P.-L.G. and C. B. performed research; P.-L.G. and C. B. wrote the paper.

The authors declare no conflict of interest.

[1]To whom correspondence should be addressed. E-mail: giscard@univ-littoral.fr and christian.bonhomme@upmc.fr

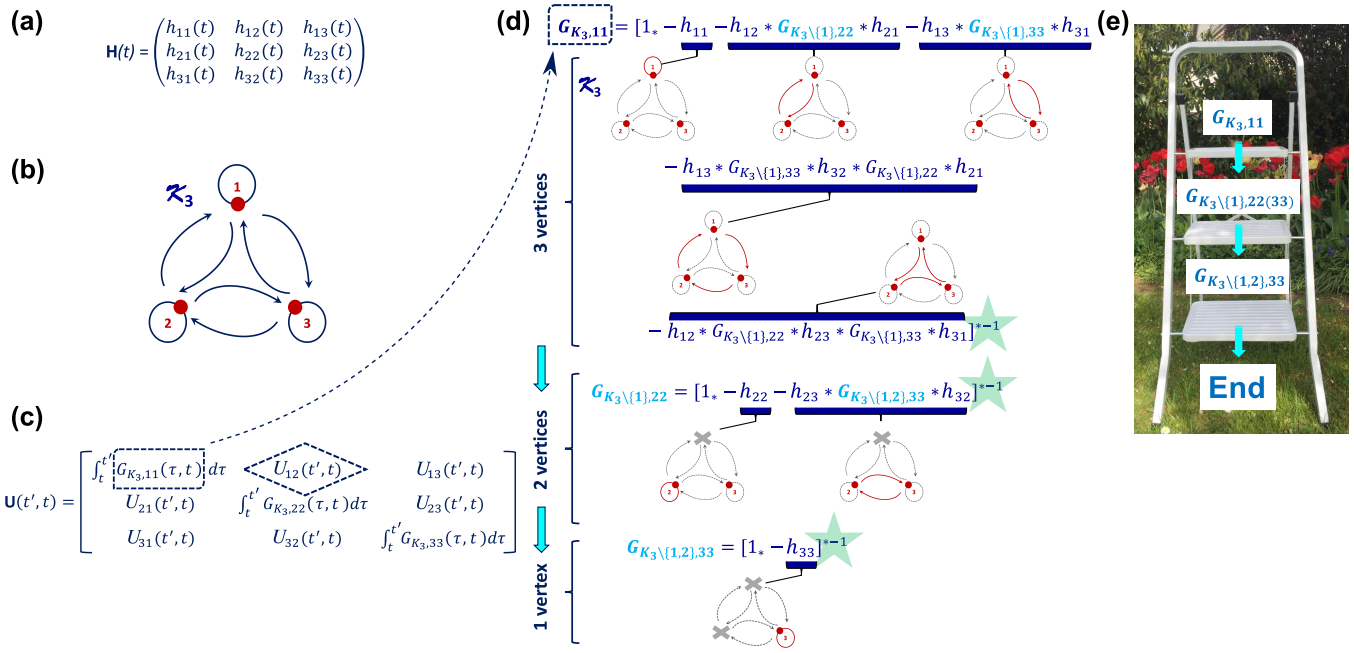

Fig. 1. The path-sum continued fraction for the exact calculation of the entries of $\mathsf{U}(t',t)$ is always of finite depth and breadth. **(a)** The illustrative example of a 3×3 time-dependent Hamiltonian $\mathsf{H}(t)$ which is involved for instance in the $I=1$ spin dynamics. **(b)** The associated dynamical graph $\mathcal{G}_t = K_3$ with adjacency matrix $\mathsf{H}(t)$. Circles correspond to self-loops (diagonal terms of $\mathsf{H}(t)$). Directed edges correspond to off-diagonal terms. The associated weights corresponds to the entries of $\mathsf{H}(t)$. **(c)** Evolution operator $\mathsf{U}(t',t)$ as seen by path-sum. The mathematical objective here is the calculation of the $G_{K_3,ii}(t',t)$ terms, which involve $*$-inverses (green stars). Path-sum then gives the off-diagonal entries of $\mathsf{U}(t',t)$ (dashed diamond) from easy $*$-products involving $G_{K_3,ii}(t',t)$ and $h_{ij}(t)$ terms, with no further $*$-inverses. For example, $U_{21} = 1 * G_{K_3\setminus\{1\},22} * h_{21} * G_{K_3,11} + 1 * G_{K_3\setminus\{1,3\},22} * h_{23} * G_{K_3\setminus\{1\},33} * h_{31} * G_{K_3,11}$. **(d)** Step by step evaluation of $G_{K_3,11}(t',t)$ (dashed square) showing the finite character of the involved continued fraction. The sum is performed on the finite cycles of length 1, 2 and 3 respectively (the corresponding walks are indicated in red—other edges are indicated in dashed grey lines). At each step of the continued fraction, a vertex is removed (see the left part of the Figure). **(e)** A pictorial representation of "descending ladder principle" for the path-sum continued fraction. The calculation starts at the top of the ladder with each $*$-inverse leading to the step below and ending in all (finite dimensional Hamiltonian) cases on the ground: the continued fraction is of finite depth.

early polarised RF excitation. It corresponds to the influence of the counter-rotating component of the RF field and the Bloch-Siegert effect. Path-sum further leads to exact and compact representations of recently uncovered special solutions involved in two levels quantum dynamics, namely confluent Heun's functions otherwise known in general relativity and astrophysics (28), see SI. The two final examples are related to many-body Hamiltonians, including N like-spins coupled by the homonuclear dipolar coupling and spin diffusion under MAS. In this later case, it is demonstrated that if the initial density matrix $\rho(0)$ is a pure state with a small number $k \ll N$ of up-spins, the evolution of $\rho(t)$ can be made analytically, even in the limit $N\to\infty$. The effects of MAS frequency and chemical shift offsets will be illustrated on an organometallic molecule exhibiting 42 protons. We emphasize the fact that all simulations presented below, including the animations, typically took *a minute* to be generated on a standard laptop. More theoretical results related to spin chains are presented in the SI.

Quantum evolution and walks on graphs

Quantum systems with exclusively discrete degrees of freedom such as spin systems, obey a discrete analog to Feynman's path integrals. To illustrate this, define one history of a quantum system as a temporal succession of *orthogonal* quantum states $h \;:\; |s_1\rangle \mapsto |s_2\rangle \mapsto |s_3\rangle \cdots$, each transition $|s_i\rangle \mapsto |s_{i+1}\rangle$ happening at a specified time t_i. Overall the history h acquires a complex weight which is the product of the weights of all the transitions in the history. The weight of an individual transition $|s_i\rangle \mapsto |s_{i+1}\rangle$ is dictated by the Hamiltonian as $\langle s_{i+1}|\mathsf{H}(t_i)|s_i\rangle$.

A natural representation of such discrete histories is as walks on a graph. To see this, let $\mathcal{G}_t$ be the graph such that each vertex v_i corresponds to one member $|s_i\rangle$ of an orthonormal basis for the entire state-space and give the directed edge $v_i \mapsto v_j$ the *time-dependent* weight $\langle s_j|\mathsf{H}(t)|s_i\rangle$. In this picture, a system history as defined earlier is a walk on $\mathcal{G}_t$ and $\mathsf{H}(t)$ is the adjacency matrix of $\mathcal{G}_t$. Because the Hamiltonian is time-dependent, the graph itself is dynamical, see Fig 1(a,b) for an example.

General solution. Now just as for Feynman's path-integrals, the exact evolution of the system is obtained from the superposition of all its possible histories. Equivalently, every element $\langle s_j|\mathsf{U}(t)|s_i\rangle$ of the evolution operator $\mathsf{U}(t)$ is given by the sum over all walks from v_i to v_j on $\mathcal{G}_t$, including all possible jumping times for each transition between vertices. While individual walks are the discrete counterpart of Feynman diagrams, their algebraic structure is much better understood. This permits exact resummations of infinite families of walks to be performed at the formal level, yielding every $\langle s_j|\mathsf{U}(t)|s_i\rangle$ as a branched continued fraction that is *finite* in both depth and breadth. In particular, because this fraction comprises a finite number terms, it is unconditionally convergent when calculated numerically. The same principles apply regardless of whether the Hamiltonian depends on time or not, in the former case however the theory relies on two-times functions $f(t',t)$ that multiply via a convolution-like product

$$\big(f * g\big)(t',t) := \int_t^{t'} f(t',\tau)g(\tau,t)\,d\tau.$$

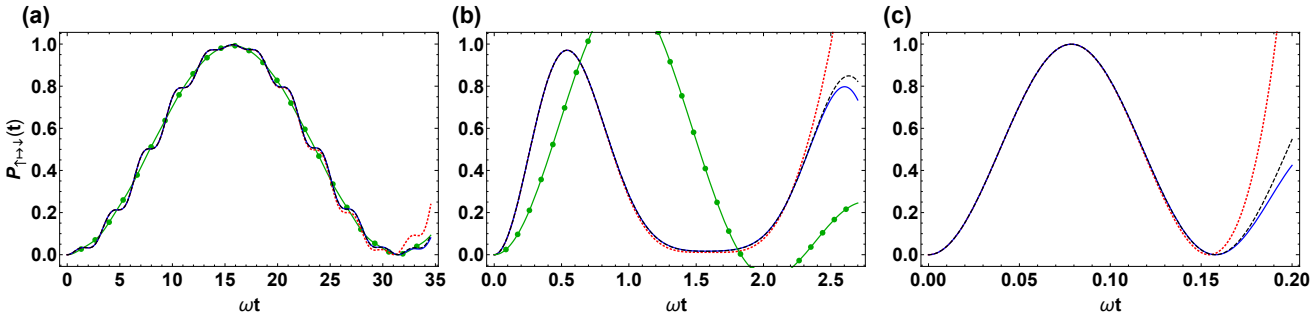

Fig. 2. Bloch-Siegert dynamics. Transition probability $P_{\uparrow\mapsto\downarrow}(t)$ as a function of time in **(a)** the weak, **(b)** mid and **(c)** strong coupling regimes. Shown here are the results from second order Floquet theory (16) (solid green line and green points); and second (dotted red lines) and third orders (solid blue line) of the Neumann series for transition amplitude $A_{\uparrow\mapsto\downarrow}$ calculated analytically from the path-sum result. The Floquet result is not shown on figure **(c)** where it oscillates erratically and would make the plot unreadable. The exact numerical solution (dashed black line) is indistinguishable from the fourth Neumann order for $A_{\uparrow\mapsto\downarrow}$. Parameters : two level system driven by the resonant $\omega_0 = \omega$ Bloch-Siegert Hamiltonian of Eq. [8] (16, 17) starting in the $|\uparrow\rangle$ state at $t = 0$, $b/\omega_0 = 1/10$ (left figure), $b/\omega_0 = 3/2$ (middle figure) and $b/\omega_0 = 10$ (right figure).

This means that for general time-dependent Hamiltonians the continued fraction formulation for $\mathsf{U}(t)$ involves products and inverses with respect to the $*$ multiplication. Such $*$-inverses are solutions to linear Volterra equations of the second kind and can be always expressed analytically by super-exponentially convergent Neumann series.

While the rigorous mathematics underpinning these observations were laid out in (26, 29) within the more general framework of systems of coupled linear differential equations with non-constant coefficients, no concrete physical applications were presented. In view of the paucity of mathematical methods to calculate quantum dynamics driven by time-dependent Hamiltonians and the general lack of fundamental progress on the theory since Magnus' work in 1954 (5); it appears essential to introduce path-sums to the physics community via illustrative examples bearing on currently open problems. We focus on NMR in the following.

Two-level time-dependent Hamiltonians

Two-level systems driven by time-dependent Hamiltonians continue to be a very active area of research (11, 30–33) owing to their experimental relevance; their role as theoretical models; and the need to master the internal dynamics of qubits undergoing quantum gates (31, 34). The most general two-level Hamiltonian is

$$\mathsf{H}(t) = \begin{pmatrix} h_\uparrow(t) & h_{\uparrow\downarrow}(t) \\ h_{\downarrow\uparrow}(t) & h_\downarrow(t) \end{pmatrix}. \qquad [2]$$

In this expression we only require that $h_{\downarrow\uparrow}(t)$, $h_{\uparrow\downarrow}(t)$, $h_\uparrow(t)$ and $h_\downarrow(t)$ be bounded functions of time over the interval $[t, t']$ of interest. So far, no analytical expression has been found for the corresponding evolution operator $\mathsf{U}(t)$ defined as the *unique* solution of Eq. [1] with the Hamiltonian of Eq. [2]. It is known that particular choices for $\mathsf{H}(t)$ lead to evolution operators that involve higher special functions, e.g. Heun's functions (30) see SI for more details. Thus *the best possible result* for the general $\mathsf{U}(t)$ is that each of its entries be described as solving a defining equation, and that an *analytical* mean of generating this solution be presented. This is precisely what path-sums achieve:

$$\mathsf{U}(t', t) = -i\times \qquad [3]$$
$$\begin{pmatrix} i(1 * G_\uparrow) & 1 * F_\uparrow * h_{\uparrow\downarrow} * G_\downarrow \\ 1 * F_\downarrow * h_{\downarrow\uparrow} * G_\uparrow & i(1 * G_\downarrow) \end{pmatrix},$$

where $F_\uparrow := (\delta + h_\uparrow e^{-i(1*h_\uparrow)})$ and similarly for $F_\downarrow$ with δ the Dirac delta function. The two-times Green's functions $G_\uparrow$ and $G_\downarrow$ solve linear Volterra equations of the second kind, e.g. for $G_\uparrow$ we have $G_\uparrow = \delta + K_\uparrow * G_\uparrow$, that is

$$G_\uparrow(t', t) = \delta(t', t) + \int_t^{t'} K_\uparrow(t', \tau)\, G_\uparrow(\tau, t)\, d\tau, \qquad [4]$$

where $K_\uparrow = -ih_\uparrow - h_{\uparrow\downarrow} * F_\downarrow * h_{\downarrow\uparrow}$ is called the kernel of the Volterra Eq. [4].

It is a general feature of path-sums that the kernel functions appearing in the calculations are *separable* (also called *degenerate*), that is they can always be written as sums of products of functions of a single time variable $K(t', t) = \sum_{i=1}^{q} A_i(t')B_i(t)$. This property holds true for general N-body Hamiltonians and facilitates the analysis of the Volterra equations from path-sums (35). Should a closed form expression for the solution nonetheless be out of reach, the solution is at least analytically available as a Neumann series; in the case Eq. [4] it is $G_\uparrow = \delta + \sum_{n>0} K_\uparrow^{*n}$. If every entry of the Hamiltonian is a bounded function of time, this series representation converges super-exponentially and uniformly (26). Alternatively, Volterra equations can also be solved fully numerically (36).

An expression of $\mathsf{U}(t', t)$ (Eq. [3]) where all $*$-products have been explicited with integrals as well as the demonstration that $K(t', t)$ is always separable is given in SI.

Test-model: failure of Magnus series and Floquet theory. As a first example of application for the general analytical form of Eq. [3] for the evolution operator, we take (13)

$$\mathsf{H}(t) = \frac{1}{2}\omega_0\sigma_z + \beta\big(\sigma_x \cos\omega t + \sigma_y \sin\omega t\big), \qquad [5]$$

with $\sigma_{x,y,z}$ the Pauli-matrices, and ω_0, ω and β are real parameters. This Hamiltonian, which represents a two-level atom subjected to a time-dependent circularly polarised radio-frequency field, is an important test model (37). Indeed, by transforming into a rotating frame the evolution operator is found exactly. Back in the non-rotating frame it is

$$\mathsf{U}(t) = \exp\Big(-\frac{1}{2}i\omega t\,\sigma_z\Big)\exp\Big(-it\Big(\frac{1}{2}(\omega_0 - \omega)\sigma_z + \beta\,\sigma_x\Big)\Big), \qquad [6]$$

neither Magnus series nor Floquet Theory can obtain this result. Furthermore, Magnus series are rigorously known to diverge here whenever $t \geq 2\pi/\omega_0$ (13, 38).

At the opposite, the evolution operator of Eq. [3] not only yields the exact analytical form of Eq. [6], but even when used

numerically it is unconditionally convergent. Furthermore, the transformation into the rotating frame is not necessary for the exact application of path-sum. See SI for a full derivation of Eq. [3] from Eq. [6]. Path-sum is thus the only *general purpose* approach capable of solving this test model.

Beyond the Rotating Wave Approximation: Bloch-Siegert dynamics. The Bloch-Siegert Hamiltonian, here denoted $\mathsf{H}_{BS}(t)$, is possibly the simplest model to exhibit non-trivial physical effects due to time-dependencies in the driving radio-frequency fields. This Hamiltonian reads

$$\mathsf{H}_{BS}(t) = \begin{pmatrix} \omega_0/2 & 2\beta\cos(\omega t) \\ 2\beta\cos(\omega t) & -\omega_0/2 \end{pmatrix}. \qquad [7]$$

Although this is not required by the path-sum method, we pass in the interaction picture to alleviate the notation, yielding

$$\mathsf{H}_{BS}(t) = 2\beta\cos(\omega t)\cos(\omega_0 t)\sigma_x + 2\beta\cos(\omega t)\sin(\omega_0 t)\sigma_y. \quad [8]$$

In these expressions, the coupling parameter β is the amplitude of the radio-frequency field. Of particular interest for qubit-driving experiments is the evolution of the transition probability $P_{\uparrow\mapsto\downarrow}(t) := |A_{\uparrow\mapsto\downarrow}(t)|^2$ between the two levels (34, 39). This quantity is usually found perturbatively using Floquet theory (16) as Magnus series again suffer from divergences (40). The result of Eq. [3] yields the probability amplitude $A_{\uparrow\mapsto\downarrow}(t)$ as the solution of the Volterra equation $A_{\uparrow\mapsto\downarrow} = F + K * A_{\uparrow\mapsto\downarrow}$ where the function F and kernel K are given in the SI. This equation has no closed form solution, that is, its solution is an hitherto unknown higher transcendental special function. We plot on Fig. (2) the transition probability $P_{\uparrow\mapsto\downarrow}(t)$ as calculated analytically from the second and third orders of the Neumann series $A_{\uparrow\mapsto\downarrow} = F * (\delta + \sum_{n>0} K^{*n})$ in the resonant case $\omega_0 = \omega$. This situation was chosen because: i) it is mathematically the most difficult to approach exactly (see SI); and ii) it yields compact expressions more suitable for a concise presentation. Higher order terms of the Neumann series are readily and analytically available, enabling precise evaluation of $P_{\uparrow\mapsto\downarrow}(t)$ at any desired target time. The fact that the same expression for $P_{\uparrow\mapsto\downarrow}(t)$ is a good approximation to the exact transition probability in all parameter regimes, i.e. from $\beta/\omega_0 \ll 1$ to $\beta/\omega_0 \gg 1$ is a signature that the path-sum approach is non-perturbative. At the opposite, Floquet theory, which is inherently perturbative, only works for $\beta/\omega \ll 1$ (16). See SI for complete calculations related to the Bloch-Siegert Hamiltonian.

$N>2$-level Hamiltonians. The path-sum approach is by no mean limited to two-level systems: e.g. solutions to all time-dependent 3×3 and 4×4 Hamiltonians are readily available and will be presented in a future work. As an example, the construction of the finite path-sum continued fraction is detailed in Fig. 1 for a complete 3×3 matrix. Note how the number of steps in the exact solution is finite because of the descending ladder principle. Generally, as long as the system is finite, any entry of the evolution operator is given by a finite number of $*$-inverses and we are only limited here by the growth of the path-sum continued fraction, itself controlled by the structure of the Hamiltonian.

For many body systems $N \gg 1$, a further problem appears, namely the exponential growth in the size of the Hamiltonian. While path-sum does not, in itself, solve the challenges posed by this well-known scaling, it offers tools to manage it via its scale invariance properties, to which we now turn.

Scale invariance

Principles. Path-sums stem from formal resummations of families of walks. This principle does not depend on what those walks represent. In particular, it remains unchanged by the nature of the evolving system. To exploit this observation, consider a more general type of system histories made of temporal successions of orthogonal vector spaces $\tilde{h}: V_1 \mapsto V_2 \mapsto \cdots$. Physically such histories can describe an evolving subsystem, such as a cluster of particles. Mathematically they correspond to walks on a coarse-grained representation of the quantum state space, a subgraph $\tilde{\mathcal{G}}_t$ of $\mathcal{G}_t$. To see this, take a complete family of orthogonal spaces, i.e. $\bigoplus_{i=1} V_i = V$, where V is the entire quantum state space. To each V_i associate a vertex v_i and give the edge $v_i \mapsto v_j$ the time-dependent weight $\mathsf{P}_{V_j}.\mathsf{H}(t).\mathsf{P}_{V_i}$. Here P_{V_k} is the projector onto V_k. Observe then that these edge weights are generally non-Abelian. Yet, because path-sums fundamentally retain the order and time of the transitions in histories when performing resummations of walks, this setup poses no further difficulty. It follows that the submatrix $\mathsf{P}_{V_j}.\mathsf{U}(t',t).\mathsf{P}_{V_i}$ of the evolution operator is again given as a matrix-valued branched continued fraction of finite depth and breadth. While the shape of this fraction depends on the particular choice of vector spaces, its existence and convergence properties do not. If the vector spaces are chosen so that the shape of the fraction itself is unchanged, and such a choice is always possible, then the path-sum formulation is truly invariant under scale changes in the quantum state space.

An immediate consequence of scale-invariance is that there is always a path-sum calculation rigorously relating the global evolution of a system to that of any ensemble of its subsystems, such as clusters of spins in a large molecule (see below). In this scheme, we can evolve each subsystem *separately* from one-another using any preferred method (Magnus, Floquet, path-sum, Zassenhaus for short times etc.); only to then combine these isolated evolutions *exactly* via a path-sum to generate the true system evolution. In particular, if we partition the system into exactly two subsystems, the above procedure yields the time-dependent Dyson equation which forms the starting point of nonequilibrium dynamical mean-field theory (26, 41). Mathematically speaking, this situation corresponds to summing matrix-valued walks on a graph $\tilde{\mathcal{G}}_t$ with only two vertices.

Another consequence of scale invariance is a fully rigorous justification of state-space reduction techniques for time-dependent Hamiltonians (42). More precisely, the path-sum representation of evolution operators shows that the norm of any $\mathsf{P}_{V_j}.\mathsf{U}(t',t).\mathsf{P}_{V_i}$ decays exponentially or super-exponentially with the distance between v_i and v_j on $\tilde{\mathcal{G}}_t$, depending on whether $\tilde{\mathcal{G}}_t$ has bounded degree or not (26). While thorough exploitation of the scale-invariance property is beyond the scope of this work, we demonstrate below how it can be used to tackle many-body Hamiltonians, with an emphasis on examples from NMR, i.e. spins coupled by the homonuclear dipolar interaction and spin diffusion under MAS.

Many-body Hamiltonians

Large molecule in NMR. We now turn to the general problem of determining the temporal dynamics of spin diffusion as

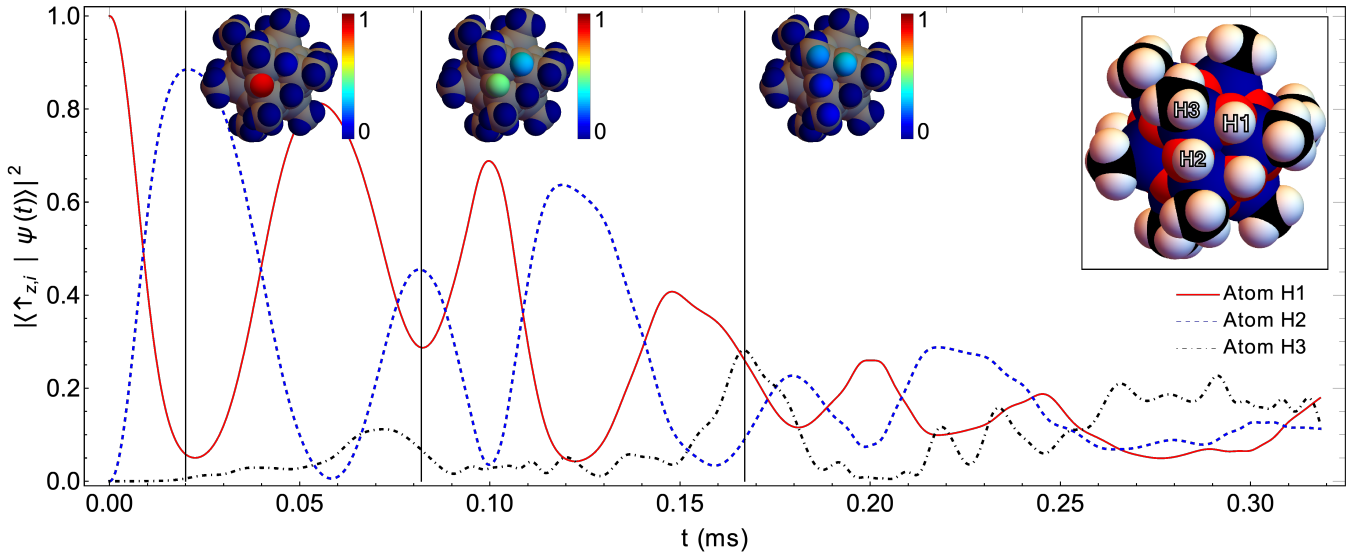

Fig. 3. Analytical spin-diffusion on a cationic tin oxo-cluster with $N = 42$ protons (shown in inset) submitted to the time-dependent high-field dipolar Hamiltonian under MAS (rotor angular velocity $\omega_r = 2\pi \times 10$kHz). The figure shows the time evolution of the probability $|\langle\psi(t)|\uparrow_{z,i}\rangle|^2$ of finding a spin-up along z on proton i for three protons: a hydroxyl proton H1 (solid red line), on which the excitation starts; a nearby hydroxyl proton H2 (dashed blue line); and a methyl proton H3 (dot-dashed black line).

effected by the time-dependent high-field dipolar Hamiltonian for N homonuclear spins:

$$\mathsf{H}^{II} = \sum_{i,j} \frac{1}{2}\omega_{ij}(t)\big(3I_{iz}I_{jz} - 2\,\mathsf{I}_i\,.\,\mathsf{I}_j\big), \qquad [9]$$

where the interaction amplitude $\omega_{ij}(t)$ is time-dependent due to the MAS rotation, see SI for more details. We consider a cationic tin oxo-cluster $\left[(\mathrm{MeSn})_{12}\mathrm{O}_{14}(\mathrm{OH})_6\right]^{2+}$ (43) exhibiting $N = 42$ protons belonging to hydroxyl and methyl groups, see Fig. 3. This structure is idealised and exhibits the main characteristics of already synthesised clusters (distances, angles, crystal packing). All atomic coordinates as well as selected internuclear distances are given in *SI*. The methyl groups are supposed fixed as is the case at low temperature. A single orientation of the molecule towards the principal magnetic field B_0 is considered, while the extension to a powder could be easily obtained by using averaging procedures over the crystallites (44) or an expression derived from a Fokker-Planck equation (45).

Path-sum yields analytical expressions for the entries of the evolution operator because the computational complexity of the calculations can be made to be only linear in the system size N depending on the initial state. We stress that this is due primarily to the peculiar structure of the high-field dipolar Hamiltonian, which allows for a particularly efficient usage of the scale-invariance and graphical nature of path-sums. In particular, we do not claim to have solved the general many-body problem: there will be Hamiltonians for which this procedure cannot circumvent the exponential explosion of the state space.

In Fig. 3 and Animation 1 (supplementary material), ω_r is fixed at $2\pi \times 10$ kHz and the initial up-spin is located on a hydroxyl proton, denoted H1. During the first 0.15ms time period (or 1.5 rotor period), an oscillation is observed between two close hydroxyl protons H1 and H2, followed by a partial transfer to the closest methyl group ($t \gtrsim 0.15$ms), in particular proton H3. Inside the methyl entity, the frequency of exchange is much faster as the three protons are subjected to much stronger dipolar couplings. In Fig. 4(a,b) and Animations 2, 3, 4 and 5 for $\omega_r = 20$, 40, 60 and 120 kHz, the return-probability to spin 1 is expressed as a function of ω_r and can be described analytically. These results provide an exact justification to recently proposed approximations in the context of the ^{1}H line dependence under ultra-fast MAS (46). Finally in Fig. 4(c), strong offsets (roughly 30 ppm at 1.5 GHz, currently the highest magnetic field available for high resolution solid state NMR purposes) were added to all protons H_i, except the two hydroxyl protons $\mathrm{H}_{1,2}$ (see inset of Fig. 3 for identification). As the chemical shift offset corresponds simply to $I_{z,i}$ operators, the solution of the spin diffusion problem remains analytical by using path-sum. For strong offsets, spin diffusion is quenched. All of these results are in perfect agreement with experimental observations related to spin diffusion in NMR.

Methodology: setting up the path-sum.

Considerations on the initial state. The key is to choose the initial density matrix $\rho(0)$ to be a pure state with a small number k of up- or down-spins. Indeed, since the high-field Hamiltonian of Eq. [9] conserves this number at all times, the discrete graph structure $\mathcal{G}_t$ encoding the quantum state space for path-sum consists of exactly N disconnected components, of sizes $\binom{N}{k} \sim N^k$ when $k \ll N$. Hence, the computational cost of finding the evolution operator using a path-sum here is $O\big(N^k\big)$, i.e. *linear* in N for a single initial up-spin. This procedure is different from approximate state space truncations approaches (23, 24, 47), since here the Hamiltonian rigorously enforces the state-space partition. As a result, our calculations retain quantum correlations of up to N spins. More general initial density matrices $\rho(0)$ may be approximated with polynomial cost on expanding them over pure states with $k \ll N$. In the sector of the quantum space with a single up-spin, the difficulty is thus solely due to the time-dependent nature of the Hamiltonian. The evolution operator is then strictly analytical for static experiments and analytically soluble using path-sums for MAS experiments. Physically, the time-dependent high-field dipolar Hamiltonian of Eq. [9] implements a continuous time quantum random walk of the spin on the molecule. This interpretation remains true in the presence of more than one

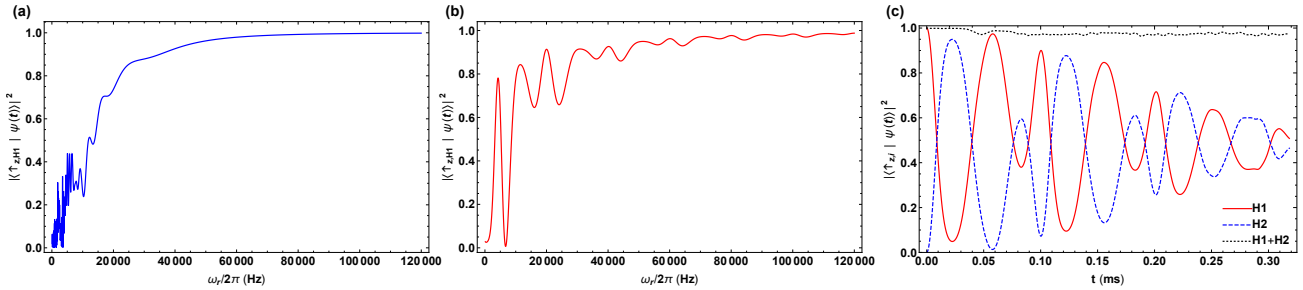

Fig. 4. Return probability for the spin excitation on the initial hydroxyl proton H1 as a function of ω_R (one plot point every 20Hz): **(a)** after a fixed time of $t = 0.05$ms, a situation exhibiting numerous peaks for small ω_R values that are not all resolved on this picture; and **(b)** after two rotor periods $t = 2 \times (2\pi/\omega_R)$. **(c)** Probability of finding the spin excitation on hydroxyl protons H1 (solid red line) or H2 (dashed blue line) as a function of time for $\omega_R = 10$kHz and with a very strong offset of roughly 30 ppm at 1.5 GHz on all protons except H1 and H2. The total probability of being either on H1 or H2 (dotted black line) never goes below $\simeq 0.94$ over 3 rotor periods.

initial up-spin, with the caveat that further interactions happen when quantum walkers meet. Preliminary observations related to spin chains (see SI) suggest that the results obtained by starting from a pure state initial density matrix give a very good first approximation to more general initial mixed states, as usually encountered in standard room temperature NMR. This particular point will be studied in-depth in a separate work.

Dynamics at the molecular scale. As stated above, the sector of the quantum state space that needs to be considered for an initial pure state with a single up-spin is of dimension N. This observation reduces the problem of calculating the evolution operator to (analytically) solving an $N \times N$ system of coupled linear differential equations with non-constant coefficients. Since, in principle, all pairs of spins interact *directly*, this system is full. Consequently, if no further partition of the Hamiltonian is used, the graph $\mathcal{G}_t$ on which path-sum is to be implemented is the complete graph on N vertices, which entails a *huge* (yet finite) number of terms in the path-sum continued fraction. The vast majority of these give negligible contributions to the overall dynamics however, because of the scales of the interactions involved: one may therefore build up the path-sum continued fraction by brute force, progressively including longer cycles until convergence of the solution is obtained.

An alternative, physically motivated approach appealing once more to scale-invariance nonetheless appears preferable as it yields further insights in the temporal dynamics. First, remark that at least one further non-trivial partition of the Hamiltonian is quite natural in the case of the cationic tin oxo-cluster: that which puts together all spins belonging to the same methyl or 3 hydroxyls groups. Mathematically, this is equivalent to seeing the Hamiltonian as a 14×14 matrix with matrix valued entries, each of size 3×3. Then there is a path-sum continued fraction expressing any 3×3 block of the the global evolution operator $\mathsf{U}(t', t)$ in terms of the "small" Hamiltonians of the corresponding proton groups.

At this point the path-sum continued fraction is already quite manageable without further approximations, but we can gain additional (analytical!) insights into the spin dynamics by removing inter-group interactions weaker than a chosen cut-off value $I_{B,B'}/\Lambda$, with $I_{B,B'}$ the maximum inter-group interaction. Here B indices mean "block". The value of Λ is itself controlled by convergence of the overall solution. This procedure sends some off-diagonals blocks of the Hamiltonian to 0, giving $\tilde{\mathcal{G}}_t$ a non-trivial topology which reveals the molecular structure at the methyl and 3 hydroxyls scale, as experienced by the spin excitation during diffusion. See Fig. (5) for an illustrative example, with $\omega_r = 2\pi \times 60$ kHz and $\Lambda = 40$. The corresponding path-sum continued fraction takes on the topology of the molecule, can be evaluated analytically, and establishes mathematically the main pathways taken by the spin excitation:

$$\begin{aligned}\mathsf{U}_{(\mathrm{OH})_3} = 1 * \Big(&\mathsf{Id}_* + i\mathsf{H}_\mathrm{H} + \mathsf{H}_\mathrm{HM} * \Sigma_1 * \mathsf{H}_\mathrm{MH} + \mathsf{H}_\mathrm{HM} * \Sigma_2 * \mathsf{H}_\mathrm{MH} \\ &+ \mathsf{H}_\mathrm{HM} * \Sigma_4 * \mathsf{H}_\mathrm{MH} - i\,\mathsf{H}_\mathrm{HM} * \Sigma_2 * \mathsf{H}_\mathrm{MM} * \Sigma_1 * \mathsf{H}_\mathrm{MH} \\ &- i\,\mathsf{H}_\mathrm{HM} * \Sigma_4 * \mathsf{H}_\mathrm{MM} * \Sigma_2 * \mathsf{H}_\mathrm{MH}\Big)^{*-1},\end{aligned}$$

where the Σ_j are given by

$$\begin{aligned}\Sigma_1 &= \frac{1}{\mathsf{Id}_* + i\mathsf{H}_\mathrm{M} + \mathsf{H}_\mathrm{MM} * \Sigma_2 * \mathsf{H}_\mathrm{MM}}, \\ \Sigma_2 &= \frac{1}{\mathsf{Id}_* + i\mathsf{H}_\mathrm{M} + \mathsf{H}_\mathrm{MM} * \Sigma_3 * \mathsf{H}_\mathrm{MM}}, \\ \Sigma_3 &= \frac{1}{\mathsf{Id}_* + i\mathsf{H}_\mathrm{M} + \mathsf{H}_\mathrm{MM} * \Sigma_4 * \mathsf{H}_\mathrm{MM}}, \\ \Sigma_4 &= \frac{1}{\mathsf{Id}_* + i\mathsf{H}_\mathrm{M}},\end{aligned}$$

illustrating once more the descending ladder principle evoked in Fig. (1). Here, all inverses are $*$-inverses and $\mathsf{U}_{(\mathrm{OH})_3}$ is the 3×3 block of the global evolution operator giving the probability amplitudes over a group of 3 hydroxyls. H_M and H_H are the Hamiltonians of isolated methyl and of a group of 3 hydroxyls, respectively. Similarly, H_MM is the interaction between neighbouring methyls and $\mathsf{H}_\mathrm{MH} = \mathsf{H}_\mathrm{HM}$ the interaction between a methyl and a group of 3 hydroxyls.

The perspicacious reader may notice that the shape taken by the continued fraction for $\mathsf{U}_{(\mathrm{OH})_3}$ is immediately related to that of the graph $\tilde{\mathcal{G}}_t$ (Fig. 5(b)), with each term of the fraction being the weight of a fundamental cycle of the graph. This close, transparent, association between the mathematical form of the solution and the physical problem allows for physically motivated and better controlled approximations. For example, setting Σ_3 to the identity in the above solution is immediately understood to mean that one removes the possibly for the spin to diffuse to the remote methyl groups Me5 and Me6 before coming back to the initial group of 3 hydroxyls, an excellent approximation (see Fig. 5(a), red points to be compared to the red dashed line)!

Finally, we remark that our choice of partition is not mathematically necessary. For example, larger blocks may be employed equally well or one may form blocks with protons scattered throughout the molecule. In principle, path-sum's

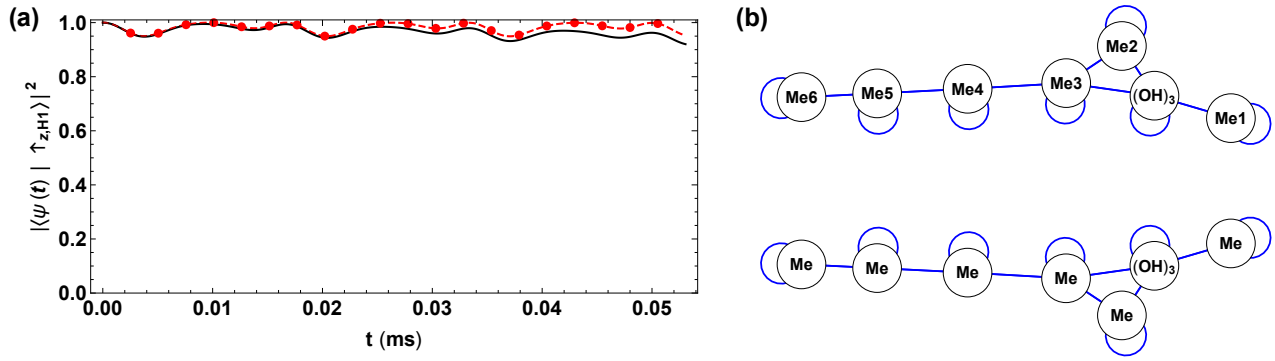

Fig. 5. Building the path-sum on the cationic tin oxo-cluster. (a) Probability of return of the spin excitation on a hydroxyl proton H1 as a function of time for $\omega_r = 2\pi \times 60$ kHz over 3 rotor periods: (i) exact solution (solid black line, identical with $\Lambda > 100$), (ii) approximation with low interaction cut-off $\Lambda = 40$ (dashed red line) and (iii) further approximation obtained upon setting Σ_3 to the identity (red points). **(b)** Discrete structure $\tilde{\mathcal{G}}_t$ of the quantum state space as seen by path-sum when $\Lambda = 40$ and corresponding to the equations given in the text for $U_{(OH)_3}$. Edges and self-loops correspond to inter-and intra-group interactions, respectively. The adjacency matrix of this graph is the 14×14 Hamiltonian with matrix valued entries evoked in the text. Thus, the shape of the graph is essentially that of the molecule at the methyl and group of 3 hydroxyls level. It comprises two disconnected pathways for spin diffusion corresponding to the opposite sides of the cationic tin oxo-cluster which become connected for higher cut-off values $\Lambda > 42$.

scale-invariance guarantees that any choice, if properly implemented, leads to the same solution. In practice however there is a trade-off between the size of the manipulated blocks and the complexity of the path-sum continued fraction. We do not know in general how to choose the best partition according to this trade-off but it seems that physically motivated partitions are a good starting point.

Conclusion

In this contribution, we have demonstrated an entirely novel approach to the problem of finding compact and exact expressions for the evolution operators of quantum dynamical systems driven by time-varying Hamiltonians. In fact, the potential of application of path-sum exceeds Hermitian matrices since it can be applied to any finite matrix* and even extends to infinite ones under additional assumptions such as translation invariance. As illustrated in Figure 1, path-sum calculations always involve a descending ladder of progressively simpler quantities yielding the exact solution after a finite number of steps. This is in strong contrast with traditional perturbation techniques (ME, FT), which invariably lead to infinite series and an ascending ladder of increasingly intricate quantities, such as Magnus series' nested commutators. Most importantly, the solutions provided by path-sums are always analytically accessible, e.g. through Neumann series for the $*$-inverses. Mathematically, since these solutions can involve special functions, no better form for them can in general be expected. Path-sum may alternatively be implemented fully numerically by exploiting the properties of the separable linear Volterra equations of the second kind, which the method produces. This option has not been used in this contribution.

As a fundamental and illustrative example, we used path-sum to solve the Bloch-Siegert problem—related to the action of the counter-rotating component of the radio-frequency field— at any order. We anticipate that further complex, and currently unsolved problems, involving 3×3, $4 \times 4, \cdots$, matrices will be solved using path-sums as well. As a remarquable example, the exact evolution of the macroscopic magnetisation M in a strong magnetic field B_0 under the action of any $B_1(t)$ radio-frequency field (a 3×3 problem) will be presented in a separate contribution. Relaxation and decoherence processes will be taken explicitly into account by extending path-sum to the Liouvillian space.

We analytically studied the spin diffusion effected by the homonuclear dipolar coupling Hamiltonian of NMR acting on a large molecule, starting from a pure state initial density matrix. In general, on many-body systems, we are facing two kinds of "explosive" computational problems: (i) one, quantum in nature, related to the exponential size of the quantum state space; and (ii) one, graph theoretical in nature, related to the time required to construct the path-sum continued fraction, in particular if $\mathcal{G}_t$ is large and not sparse. Issue (ii) can be managed with partitions and path-sum's scale invariance and will further be tackled in a near future with the implementation of a newly developed Lanczos path-sum method. Lanczos path-sum relies on an exact transformation of the Hamiltonian into a time-dependent tri-diagonal matrix. The first issue (i) is fundamental to quantum mechanics and its management inherently depends on the problem at hand. For the homonuclear dipolar coupling Hamiltonian, the problem is bypassed upon choosing certain initial pure states. Moreover, the scale invariance of path-sum appears to be of paramount importance here, as it allows to separately evolve chosen subsystems only to then combine all such evolutions in a globally exact way. In the case of translation-invariant spin-chains and more general Bethe lattices driven by generic long-range Hamiltonians, we show in SI that this allows path-sum to provide *fully exact* expression for the evolution operator, even in the limit $N \to \infty$, although exploiting these solutions remains a formidable challenge. An entire new field of research is now open for the NMR and wider physics communities.

ACKNOWLEDGMENTS. P.-L. Giscard is grateful for the financial support from the Royal Commission for the Exhibition of 1851 over the period 2015–2018, during which time the present research was started. C. Bonhomme thanks Dr. F. Ribot for communicating the molecular data pertaining to the cationic tin oxo-cluster.

*Technically, we need the matrix entries to be bounded functions of time over the time-interval of interest in order to guarantee super-exponential convergence of the Neumann series for the $*$-inverses (26)

1. Slichter CP (1990) *Principles of Magnetic Resonance*, Springer Series in Solid-State Sciences. (Springer-Verlag, Berlin Heidelberg), 3 edition.
2. Ernst R, Bodenhausen G, Wokaun A (1987) *Principles of Nuclear Magnetic Resonance in*

One and Two Dimensions, International series of monographs on chemistry. (Clarendon Press).
3. Mehring M, Weberruß V (2001) *Object-Oriented Magnetic Resonance*. (Academic Press, London).
4. Dyson FJ (1952) Divergence of Perturbation Theory in Quantum Electrodynamics. *Physical Review* 85(4):631–632.
5. Magnus W (1954) On the exponential solution of differential equations for a linear operator. *Communications on Pure and Applied Mathematics* 7(4):649–673.
6. Haeberlen U, Waugh JS (1968) Coherent Averaging Effects in Magnetic Resonance. *Phys. Rev.* 175(2):453–467.
7. Burum DP, Rhim WK (1979) Analysis of multiple pulse nmr in solids. iii. *The Journal of Chemical Physics* 71(2):944–956.
8. Warren WS, Weitekamp DP, Pines A (1980) Theory of selective excitation of multiple-quantum transitions. *The Journal of Chemical Physics* 73(5):2084–2099.
9. Bialynicki-Birula I, Mielnik B, Plebański J (1969) Explicit solution of the continuous Baker-Campbell-Hausdorff problem and a new expression for the phase operator. *Annals of Physics* 51(1):187–200.
10. Maricq MM (1982) Application of average hamiltonian theory to the nmr of solids. *Phys. Rev. B* 25(11):6622–6632.
11. Blanes S, Casas F, Oteo J, Ros J (2009) The magnus expansion and some of its applications. *Physics Reports* 470(5):151 – 238.
12. Moan PC, Niesen J (2008) Convergence of the magnus series. *Foundations of Computational Mathematics* 8(3):291–301.
13. Sánchez S, Casas F, Fernández A (2011) New analytic approximations based on the magnus expansion. *Journal of Mathematical Chemistry* 49(8):1741–1758.
14. Goldman M, et al. (1992) Theoretical aspects of higher-order truncations in solid-state nuclear magnetic resonance. *The Journal of Chemical Physics* 97(12):8947–8960.
15. Floquet G (1883) Sur les équations différentielles linéaires à coefficients périodiques. *Annales scientifiques de l'École Normale Supérieure* 2e série, 12:47–88.
16. Shirley JH (1965) Solution of the schrödinger equation with a hamiltonian periodic in time. *Phys. Rev.* 138(4B):B979–B987.
17. Bloch F, Siegert A (1940) Magnetic resonance for nonrotating fields. *Phys. Rev.* 57(6):522–527.
18. Vega S (1996) Floquet theory in *Encyclopedia of Nuclear Magnetic Resonance*, eds. Grant DM, Harris RK. (Wiley, New York), p. 2011.
19. Leskes M, Madhu P, Vega S (2010) Floquet theory in solid-state nuclear magnetic resonance. *Progress in Nuclear Magnetic Resonance Spectroscopy* 57(4):345 – 380.
20. Scholz I, Meier BH, Ernst M (2007) Operator-based triple-mode floquet theory in solid-state nmr. *The Journal of Chemical Physics* 127(20):204504.
21. Takegoshi K, Miyazawa N, Sharma K, Madhu PK (2015) Comparison among magnus/floquet/fer expansion schemes in solid-state nmr. *The Journal of Chemical Physics* 142(13):134201.
22. Mananga E (2018) Theoretical perspectives of spin dynamics in solid-state nuclear magnetic resonance and physics. *Journal of Modern Physics* 9:1645–1659.
23. Brüschweiler R, Ernst RR (1997) A cog-wheel model for nuclear-spin propagation in solids. *Journal of Magnetic Resonance* 124(1):122 – 126.
24. Dumez JN, Butler MC, Emsley L (2010) Numerical simulation of free evolution in solid-state nuclear magnetic resonance using low-order correlations in liouville space. *The Journal of Chemical Physics* 133(22):224501.
25. Mentink-Vigier F, Vega S, De Paëpe G (2017) Fast and accurate MAS-DNP simulations of large spin ensembles. *Physical Chemistry Chemical Physics* 19(5):3506–3522.
26. Giscard PL, Lui K, Thwaite SJ, Jaksch D (2015) An exact formulation of the time-ordered exponential using path-sums. *Journal of Mathematical Physics* 56(5):053503.
27. Feynman RP, Hibbs AR (2005) *Quantum Mechanics and Path Integrals*, Dover Books on Physics. (Dover Publications), emended by D. F. Styer edition.
28. Hortaçsu M (2018) Heun functions and some of their applications in physics. *Advances in High Energy Physics* 2018:8621573.
29. Giscard PL, Thwaite SJ, Jaksch D (2012) Continued fractions and unique factorization on digraphs. *arXiv:1202.5523*.
30. Xie Q, Hai W (2010) Analytical results for a monochromatically driven two-level system. *Phys. Rev. A* 82(3):032117.
31. Barnes E, Das Sarma S (2012) Analytically solvable driven time-dependent two-level quantum systems. *Phys. Rev. Lett.* 109(6):060401.
32. Yan Y, Lü Z, Zheng H (2015) Bloch-siegert shift of the rabi model. *Phys. Rev. A* 91(5):053834.
33. Schmidt H (2018) The floquet theory of the two-level system revisited. *Zeitschrift für Naturforschung A* 73(8):705 – 731.
34. Zeuch D, Hassler F, Slim J, DiVincenzo DP (2018) Exact Rotating Wave Approximation. *ArXiv e-prints* p. arXiv:1807.02858.
35. Pleshchinskii NB, Tagirov RR (1995) On the structure of the solutions of volterra integral equations with degenerate kernel. *Journal of Mathematical Sciences* 74(5):1268–1273.
36. Hackbusch W (1995) *Integral Equations: Theory and Numerical Treatment*. (Birkhäuser Basel).
37. Klarsfeld S, Oteo J (1989) Analytic properties of the magnus operator for two solvable hamiltonians. *Physics Letters A* 142(6):393 – 397.
38. Casas F (2007) Sufficient conditions for the convergence of the magnus expansion. *J. Phys. A: Math. Theor.* 40:15001–15017.
39. Angelo RM, Wreszinski WF (2005) Two-level quantum dynamics, integrability, and unitary not gates. *Phys. Rev. A* 72(3):034105.
40. Maricq MM (1987) Convergence of the magnus expansion for time dependent two level systems. *The Journal of Chemical Physics* 86(10):5647–5651.
41. Aoki H, et al. (2014) Nonequilibrium dynamical mean-field theory and its applications. *Rev. Mod. Phys.* 86(2):779–837.
42. Karabanov A, van der Drift A, Edwards LJ, Kuprov I, Köckenberger W (2012) Quantum mechanical simulation of solid effect dynamic nuclear polarisation using krylov-bogolyubov time averaging and a restricted state-space. *Phys. Chem. Chem. Phys.* 14(8):2658–2668.
43. Vivas-Reyes R, et al. (2002) A DFT and HF quantum chemical study of the tin nanocluster $[(RSn)_{12}O_{14}(OH)_6]^{2+}$ and its interactions with anions and neutral nucleophiles: confrontation with experimental data. *New J. Chem.* 26(9):1108–1117.
44. Edén M, Levitt MH (1998) Computation of Orientational Averages in Solid-State NMR by Gaussian Spherical Quadrature. *Journal of Magnetic Resonance* 132(2):220–239.
45. Edwards LJ, et al. (2013) Grid-free powder averages: On the applications of the Fokker–Planck equation to solid state NMR. *Journal of Magnetic Resonance* 235:121–129.
46. Sternberg U, et al. (2018) 1H line width dependence on MAS speed in solid state NMR: Comparison of experiment and simulation. *Journal of Magnetic Resonance* 291:32 – 39.
47. Butler MC, Dumez JN, Emsley L (2009) Dynamics of large nuclear-spin systems from low-order correlations in liouville space. *Chemical Physics Letters* 477(4):377 – 381.
48. Polyanin AD, Manzhirov AV (2008) *Handbook of Integral Equations*. (Chapman and Hall / CRC), Second edition.
49. Wu Y, Yang X (2007) Strong-coupling theory of periodically driven two-level systems. *Phys. Rev. Lett.* 98(1):013601.
50. Irish EK (2007) Generalized rotating-wave approximation for arbitrarily large coupling. *Phys. Rev. Lett.* 99(17):173601.
51. Grossmann F, Dittrich T, Jung P, Hänggi P (1991) Coherent destruction of tunneling. *Phys. Rev. Lett.* 67(4):516–519.
52. Ronveaux A, et al. (1995) *Heun's Differential Equations*. (Oxford University Press).
53. Gomez Llorente JM, Plata J (1992) Tunneling control in a two-level system. *Phys. Rev. A* 45(10):R6958–R6961.
54. Baxter RJ (1989) *Exactly solved models in statistical mechanics*. (Academic Press).
55. Bethe H (1935) Statistical theory of superlattices. *Proc. Roy. Soc. London Ser A* 150(6):552–575.

Supplementary Information

Two level systems: explicit expressions. We start by giving the fully explicit form for the evolution operator of a general time-dependent two-level system.

$$\mathsf{U}(t',t)_{\uparrow\uparrow} = \int_t^{t'} G_\uparrow(\tau,t)d\tau, \qquad \mathsf{U}(t',t)_{\downarrow\downarrow} = \int_t^{t'} G_\downarrow(\tau,t)d\tau,$$

$$\mathsf{U}(t',t)_{\downarrow\uparrow} = -i\int_t^{t'}\int_t^{\tau_0}\int_{\tau_1}^{\tau_0}\Big(\delta(\tau_0-\tau_2) - ih_\downarrow(\tau_0)\, e^{-i\int_{\tau_2}^{\tau_0} h_\downarrow(\tau_3)d\tau_3}\Big) \times h_{\downarrow\uparrow}(\tau_2)G_\uparrow(\tau_1,t)\; d\tau_2\, d\tau_1\, d\tau_0.$$

$$\mathsf{U}(t',t)_{\uparrow\downarrow} = -i\int_t^{t'}\int_t^{\tau_0}\int_{\tau_1}^{\tau_0}\Big(\delta(\tau_0-\tau_2) - ih_\uparrow(\tau_0)\, e^{-i\int_{\tau_2}^{\tau_0} h_\uparrow(\tau_3)d\tau_3}\Big) \times h_{\uparrow\downarrow}(\tau_2)G_\downarrow(\tau_1,t)\; d\tau_2\, d\tau_1\, d\tau_0.$$

The kernel of the linear Volterra integral equation [4] satisfied by the Green's functions $G_\uparrow$ is

$$K_\uparrow(t',t) = -ih_\uparrow(t') - \int_t^{t'}\int_{\tau_1}^{t'} h_{\uparrow\downarrow}(t')\times \Big(\delta(\tau_2-\tau_1) - ih_\downarrow(\tau_2)\, e^{-i\int_{\tau_1}^{\tau_2} h_\downarrow(\tau_3)d\tau_3}\Big)h_{\downarrow\uparrow}(\tau_1)d\tau_2 d\tau_1 \qquad [10]$$

The kernel $K_\downarrow$ of the linear Volterra integral equation satisfied by $G_\downarrow$ is obtained upon replacing up arrows by down arrows and vice-versa in the equation above.

Path-sum kernels are separable. Path-sum formulates quantum evolution operators as continued fractions, with inverses taken with respect to the $*$-product. In this context, a $*$-inverse is the solution of a linear Volterra equation of the second kind, whose kernel is itself obtained from a path-sum continued fraction. Finding closed forms for such inverses is difficult, in fact such a form do not exist if the solution is a special function. Yet, $*$-inverses are always given at all orders by an analytically calculable series, the Neumann series $\sum_n f^{*n} = (1_* - f)^{*-1}$. Its convergence is guaranteed and super-exponential, provided f is a bounded function of time over the time interval of interest (26).

Ultimately, the path-sum construction terminates at some maximum depth where the kernel of the Volterra equation to be solved is just a diagonal entry of the Hamiltonian $-i\mathsf{H}$, say $-ih_{jj}(t)$. The corresponding $*$-inverse reads

$$\Big(1_* + ih_{jj}\Big)^{*-1}(t',t) = \delta(t'-t) - ih_{jj}(t')e^{-i\int_t^{t'} h_{jj}(\tau)d\tau},$$
$$= \delta(t'-t) - ih_{jj}(t')e^{-iH_{jj}(t')} - ih_{jj}(t')e^{iH_{jj}(t)},$$

where $H_{jj}(t) := \int h_{jj}(t)dt$ designates the primitive of $h_{jj}(t)$. Observe that the $*$-inverse of $-ih_{jj}(t)$ is separable, being the sum of products of functions of t' and t. This is because $h_{jj}(t)$ itself is separable: indeed the solution of a linear Volterra equation of the second kind with separable kernel is necessarily separable (35). As a consequence, it follows by induction that any depth in the path-sum continued fraction all kernels are separable and so are all entries of any quantum evolution operator $\mathsf{U}(t',t)$.

Test model: path-sum solution. Let us start with determining the diagonal entries of the evolution operator. According to the general solution Eq. [3] and with the Hamiltonian of Eq. [5], $\mathsf{U}(t',t)_{\uparrow\uparrow}$ and $\mathsf{U}(t',t)_{\downarrow\downarrow}$ are the integrals of $G_\uparrow$ and $G_\downarrow$ respectively, while these satisfy the Volterra equations [4] with kernels

$$K_\uparrow(t',t) = \frac{\omega_0}{2i} - \frac{i\beta^2}{\omega-\omega_0/2}\left(e^{-i(\omega-\omega_0/2)(t'-t)} - 1\right),$$

$$K_\downarrow(t',t) = -\frac{\omega_0}{2i} - \frac{i\beta^2}{\omega+\omega_0/2}\left(e^{-i(\omega+\omega_0/2)(t'-t)} - 1\right),$$

both as per Eq. [10]. These Volterra equations are amenable to standard techniques (48), yielding

$$\mathsf{U}_{\uparrow\uparrow}(t) = e^{-\frac{1}{2}i\omega t}\left(\cos(\alpha t/2) + \frac{i}{\alpha}(\omega-\omega_0)\sin(\alpha t/2)\right),$$

$$\mathsf{U}_{\downarrow\downarrow}(t) = e^{\frac{1}{2}it\left(\Delta+\frac{\omega_0}{2}\right)}\left(\cos(\alpha t/2) - \frac{i}{\alpha}\left(\Delta - \frac{\omega_0}{2}\right)\sin(\alpha t/2)\right),$$

with $\alpha^2 := 4\beta^2 + (\omega-\omega_0)^2$.

Alternatively, the generic form for the nth order of the Taylor expansion in t for $G_\uparrow$ (and $G_\downarrow$) is easy to find by induction from its Neumann series. This gives surprising but equivalent forms which did not require any Volterra equation solving technique,

$$\mathsf{U}_{\uparrow\uparrow}(t) = 1 + \sum_{n=0}^{\infty}\frac{(-it\,\beta^2/\Delta)^{n+1}}{(n+1)!}\sum_{k=0}^{n+1}\binom{n+1}{k}\left(\frac{\Delta\omega_0}{2\beta^2}-1\right)^k \times {}_2F_1\left(-k,-k+n+1;-n-1;\frac{\Delta^2}{\frac{\Delta\omega_0}{2}-\beta^2}\right),$$

where $\Delta := \omega - \omega_0/2$. The entries $\mathsf{U}_{\uparrow\downarrow}$ and $\mathsf{U}_{\downarrow\uparrow}$ then follow from easy integrations as dictated by Eq. [3],

$$\mathsf{U}_{\uparrow\downarrow}(t) = -\frac{2i\beta}{\alpha}e^{-\frac{1}{2}it\left(\Delta+\frac{\omega_0}{2}\right)}\sin(\alpha t/2),$$

$$\mathsf{U}_{\downarrow\uparrow}(t) = -\frac{2i\beta}{\alpha}e^{\frac{1}{2}it\left(\Delta+\frac{\omega_0}{2}\right)}\sin(\alpha t/2).$$

These results are identical to those obtained by the rotating frame technique yielding Eq. [6].

To avoid any possible confusion that may arise from the above example, we stress the fundamentally different natures of the Neumann and Taylor series expansions of the solution. The former is always provided by path-sum, is not perturbative, unconditionally convergent and involves complicated functions of time even at its first order; while the latter is purely an expansion in powers of t and is thus limited to short times. It is provided here to illustrate the various routes leading to the solution from the $*$-inverse.

Bloch-Siegert dynamics. The kernel K and function F for which the transition amplitude $A_{\uparrow\mapsto\downarrow}$ satisfies $A_{\uparrow\mapsto\downarrow} = F + K * A_{\uparrow\mapsto\downarrow}$ in the Bloch-Siegert model are as follows

$$F(t',t) = -2i\beta\, e^{-i\omega_0 t}\cos(\omega t),$$

$$K(t',t) = \frac{4\beta^2}{\omega^2-\omega_0^2}\cos(\omega t')\left(k(t)e^{-i\omega_0(t'-t)} - k(t')\right),$$

where $k(t) = i\omega_0\cos(\omega t) + \omega\sin(\omega t)$. In spite of the apparent divergence in the resonant case $\omega\to\omega_0$, the kernel K is actually well defined in this limit where it simplifies to

$$K(t',t) = i\frac{\beta^2}{\omega_0}e^{-i\omega_0 t'}\cos(\omega_0 t')\left(e^{2i\omega_0 t'} - e^{2i\omega_0 t} + 2i\omega_0(t'-t)\right).$$

The peculiar mathematical nature of the resonant limit $\omega\to\omega_0$ is responsible for the apparence of the term $2i\omega_0(t'-t)$ proportional to time in the kernel. In spite of this, the Neumann series for the transition amplitude remains unconditionally convergent. Up to order $n = 0, 1, 2$, this series reads

$$A^{(0)}_{\uparrow\mapsto\downarrow}(t) = F(t,0),$$

$$A^{(1)}_{\uparrow\mapsto\downarrow}(t) = F(t,0)\int_0^t(\delta(\tau) + K(\tau,0)d\tau),$$

$$A^{(2)}_{\uparrow\mapsto\downarrow}(t) = F(t,0)\int_0^t\left(\delta(\tau) + K(\tau,0) + \int_0^\tau K(\tau,\tau')K(\tau',0)d\tau'\right)d\tau.$$

This yields involved but always analytically computable expressions for $P_{\uparrow\mapsto\downarrow}$, e.g. in the resonant case $\omega = \omega_0$,

$$P^{(0)}_{\uparrow\mapsto\downarrow}(t) = 4\beta^2\cos^2(\omega_0 t),$$

$$P^{(1)}_{\uparrow\mapsto\downarrow}(t) =$$

$$\frac{2\beta^2}{\omega_0^2}\cos^2(\omega_0 t)\Big(2\beta^4\omega_0 t\sin(2\omega_0 t) - 2\beta^4\omega_0 t\sin(4\omega_0 t) - \beta^4\cos(2\omega_0 t) + \beta^4$$
$$+ 4\beta^2\omega_0 t^3\Delta(t)\sin(2\omega_0 t) + 4\beta^2\omega_0^2\Delta(t) - 2\beta^2\omega_0^2\Delta(t)\cos(2\omega_0 t) + 4\beta^2\omega_0^2$$
$$+ 2\omega_0^4\Delta(t)^2\Big),$$

with $\Delta(t) := \beta^2 t^2 - 2$. We emphasise that it is only in the resonant case that powers of t appear in the Neumann series due to the form taken by the kernel K. The resulting divergence appearing in the long time limit is easily overcome with higher orders, which are always analytically calculable. The subsequent $P^{(j)}_{\uparrow\mapsto\downarrow}$ for $j \geq 2$ are indeed readily available but too cumbersome to be reported here.

Further exact solutions and special functions. A particular model of two-level system appearing in both light-matter interactions (49, 50) and solid-state physics (51) is the Hamiltonian

$$\mathsf{H}_X(t) = \frac{1}{2}(f_0 + f_1\sin\omega t)\sigma_z + \frac{\nu}{2}\sigma_x,$$

where f_0 and f_1 are real parameters controlling the amplitude of the static and oscillating components of energy bias between the two energy levels, ω is the oscillating frequency and ν the coupling strength between the two levels. Xie *et al.* (30) have recently shown that all entries of the corresponding evolution operator have analytical expressions involving Heun (bi)confluent functions. Not only does the evolution operator of Eq. [3] yields this *exact* result through the Volterra equation [4] satisfied by these functions (52); but the Volterra kernel is–to the best of our knowledge–the first explicitly known integral kernel for Heun's functions. Indeed, so far, Heun kernels have only been known through a set of *implicit* conditions.Neither Magnus series nor Floquet theory reach the exact result, see instead (53) for a perturbative treatment.

Interaction terms in the high-field dipolar Hamiltonian. We consider the time-dependent high-field dipolar Hamiltonian of Eq. [9], with interaction terms under MAS

$$\omega_{ij}(t) := \frac{\mu_0\gamma^2\hbar}{4\pi r_{ij}^3} \times \frac{1}{2}\xi_{ij}(t),$$

where r_{ij} is the distance between protons i and j and (1)

$$\xi_{ij}(t) := 2\sqrt{2}\sin(\psi_{ij})\cos(\psi_{ij})\sin(\phi_{ij} + \omega_r t)$$
$$+ \sin(\psi_{ij})^2\cos(2\phi_{ij} + 2\omega_r t).$$

In this expression, ψ_{ij} is the angle between $\vec{ij}$ and the z-axis and ϕ_{ij} is the angle between $\vec{ij}$ and the x-axis for a coordinate system fixed to the sample. Finally, ω_r is the angular velocity of the rotor.

Spin chains.

Generic Hamiltonian and arbitrary initial state. As a final example of the use of path-sum and scale invariance in a many-body setting, we consider a chain of N spins interacting via a generic long range time-dependent Hamiltonian,

$$\mathsf{H}(t) = \sum_{i,j}\left\{\mathsf{H}_i(t) + \frac{1}{2}\mathsf{Int}_{ij}(t)\right\}.$$

Here $\mathsf{H}_i(t)$ is a one-body Hamiltonian acting on spin i and $\mathsf{Int}_{ij}(t)$ stands for the interactions between spins i and j. The initial density matrix $\rho(0)$ shall also remain unconstrained. In this setting the exponential explosion of the quantum state space is unavoidable, yet path-sum can find the true global evolution operator owing to the self-similar nature of a 1D chain. The exploitation of the resulting solution remains a challenge.

In order to give to the quantum state space a non-trivial topology, we suppose that spin-spin interactions are inversely proportional to some power of the distance r_{ij} from i to j, i.e. $\mathsf{Int}_{ij}(t) \propto 1/r_{ij}^\alpha$, $\alpha > 0$. Let I be the maximum spin-spin interaction along the chain, e.g. the interaction between neighbours, and suppose that we wish to retain all *direct* spin-spin interactions larger than some cut-off value $I/(r\Lambda)^\alpha$ with Λ an integer parameter and r the distance between neighbouring spins. This guarantees that all coherences involving up to Λ spins are exactly retained while those involving more than Λ spins are approximated to within $\sim 1/\Lambda$ of their true amplitude. Setting all interactions weaker than the cut-off to 0 naturally partitions the systems into blocks of Λ spins, which only interact with the neighbouring blocks. This procedure relates the structure of the quantum state space with that of the 1D lattice.

To set up the path-sum process, define

$$\mathsf{H}_{B_k} := \sum_{i,j\in B_k}\left\{\mathsf{H}_i(t) + \frac{1}{2}\mathsf{Int}_{ij}\right\},$$

$$\mathsf{Int}_{B_k,B_{k'}} := \sum_{i\in B_k, j\in B_{k'}}\frac{1}{2}\mathsf{Int}_{ij}(t).$$

H_{B_k} is the Hamiltonian of the isolated block B_k while $\mathsf{Int}_{B_k,B_{k'}}$ denotes the interaction terms between neighbouring blocks B_k and $B_{k'}$. We can now build the global evolution operator, initialising the path-sum continued fraction on the left-most block of the finite chain. We have $\mathsf{U}(t) = 1 * \Sigma_1$ with

$$\Sigma_1 := \Big(\mathsf{Id}_* + i\mathsf{H}_{B_1}\otimes\mathsf{Id}_{\setminus B_1} \qquad [11]$$
$$+ (\mathsf{Int}_{B_1,B_2}\otimes\mathsf{Id}_{\setminus B_1,B_2}) * (\mathsf{Id}_{B_1}\otimes\Sigma_2) * (\mathsf{Int}_{B_2,B_1}\otimes\mathsf{Id}_{\setminus B_1,B_2})\Big)^{*-1},$$

where $\mathsf{Id}_{\setminus B_1}$ and $\mathsf{Id}_{\setminus B_1,B_2}$ designate the identity on all blocks except block B_1 and blocks B_1 and B_2, respectively, while Id_{B_1} is the identity on block B_1. Here, Σ_1 is the depth-1 result of the path-sum continued fraction while Σ_2 satisfies the same equation but in terms of Σ_3. Since the system has N/Λ blocks, the above recursion stops at depth N/Λ, at which point $\Sigma_{N/\Lambda} \equiv \dot{\mathsf{U}}_B$ is the derivative of the small $2^\Lambda \times 2^\Lambda$ evolution operator of a single *isolated* block. We emphasise the very peculiar nature of the construction: each time one progresses in the continued fraction, the dimension of the solution is multiplied by 2^Λ, reaching 2^N at depth N/Λ. This formulation of the evolution operator looks like that for the partition function of a 1D chain in classical physics (54), with the notable exception that path-sum intrinsically builds up a 2^N dimensional object reflecting the quantum nature of the problem.

Because of the recursive form of the solution, infinite systems which are truly invariant under block translation are even simpler to solve since all $\Sigma_i \equiv \Sigma$ are identical. Using this in the path-sum solution yields a now *non-linear* matrix-valued Volterra equation for Σ

$$\Sigma = \Big(\mathsf{Id}_* + i\mathsf{H}_B\otimes\mathsf{Id}_{\setminus B} \qquad [12]$$
$$+ (\mathsf{Int}_{B,B'}\otimes\mathsf{Id}_{\setminus B,B'}) * (\mathsf{Id}_B\otimes\Sigma) * (\mathsf{Int}_{B',B}\otimes\mathsf{Id}_{\setminus B,B'})\Big)^{*-1},$$

and $1 * \Sigma$ is the evolution operator of a semi-infinite spin chain. Remark that the above equation can only have an infinite dimensional solution as shown by the apparent dimensional mismatch between the left and right hand-sides. This is because we made no approximations beyond the interaction cut-off and the solution is of the same dimension as the quantum state space, as it should. The infinite spin chain is finally obtained upon joining two semi-infinite ones,

$$\mathsf{U} = 1 * \Big(\mathsf{Id}_* + i\mathsf{H}_B$$
$$+ \mathsf{Int}_{B,B'} * \Sigma * \mathsf{Int}_{B',B} + \mathsf{Int}_{B,B''} * \Sigma * \mathsf{Int}_{B'',B}\Big)^{*-1},$$

with Σ defined through Eq. [12]. Note that we omitted the tensor products with the identities for the sake of clarity. Exploiting such solutions is a non-trivial task but existing techniques for state-space

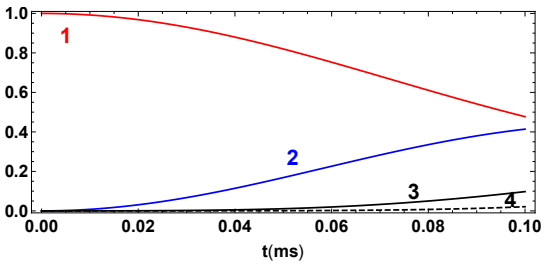

Fig. 6. Small spin chain. Probability of finding a spin up along z on a chain of 10 spins driven by the static high-field dipolar Hamiltonian ($\omega_r = 0$) as calculated by path-sum. Initially, the system is in a pure state with a single up-spin located on the left-most spin, denoted 1. Inter-spin distance of 3Å in a linear configuration.

reduction could be used. In particular, path-sum continued fractions such as Eq. [11] converge rapidly with increasing depth, see Fig (5) for an illustration of this phenomenon. Hence, stopping the recursion at depth d might yield excellent approximations. Physically, this is equivalent to truncating the system d blocks away from the central one under study.

The self-similar nature of the chain which allows for an exact formulation of the solution using path-sum generalises to systems that are Bethe lattices by blocks. These lattices, which vaguely resemble dendrimer molecules, are well known to approximate infinite regular spin lattices $\mathbb{Z}^d$ in classical statistical physics (54, 55). The ideas expounded here encourage us to develop a systematic way of mapping quantum Hamiltonians onto linear chains, irrespectively of the real geometry of the underlying physical system. This is achieved by a path-sum based Lanczos-like method for time- and path-ordered exponentials, which requires some novel mathematical notions and will thus be presented in a separate work. Of course this approach does not in itself solve the issues related to the exponential size of the quantum state space, which must be tackled via separate approximations.

High-field dipolar Hamiltonian. The equations given above for the generic spin chain apply to the high-field dipolar Hamiltonian acting on a chain of protons. If we further assume the initial state to be a pure state with a single up- or down-spins, we can focus on the corresponding sector of the quantum state space which is of linear dimension. This does not change the generic solution determined above: rather it allows us to trim it from an exponentially large evolution operator to only the relevant piece of it, of size $N \times N$.

We studied analytically a linear chain of 10 spins with no interaction cut-off (i.e. retaining all interactions) in order to compare the evolution of the pure initial state with that of the mixed state used in the literature $\rho(0) = I_{1z}/\mathrm{Tr}(I_{1z}^2)$. The results, shown in Fig. (6), illustrate the close proximity of the evolutions of the pure and mixed initial states (compare with Fig. 2 of (23)). This encourages further research on approximating mixed initial states from superpositions of pure states with small number of up- or down-spins when studying systems driven by the high-field dipolar Hamiltonian.